Stochastic Lighthill-Whitham-Richards traffic flow model for nonlinear speed-density relationships

Tianxiang Fan, S.C. Wong, Zhiwen Zhang & Jie Du

View supplementary material

Published online: 29 Oct 2024.

Submit your article to this journal

Article views: 111

View related articles

View Crossmark data

Taylor & Francis
Taylor & Francis Group

 OPEN ACCESS Check for updates

Stochastic Lighthill-Whitham-Richards traffic flow model for nonlinear speed-density relationships

Tianxiang Fan[a], S.C. Wong[a], Zhiwen Zhang[b] and Jie Du[c,d,e]

[a]Department of Civil Engineering, The University of Hong Kong, Hong Kong SAR, People's Republic of China; [b]Department of Mathematics, The University of Hong Kong, Hong Kong SAR, People's Republic of China; [c]School of Mathematical Sciences, East China Normal University, Shanghai, People's Republic of China; [d]Shanghai Key Laboratory of PMMP, East China Normal University, Shanghai, People's Republic of China; [e]Key Laboratory of MEA (Ministry of Education), East China Normal University, Shanghai, People's Republic of China

ABSTRACT

Stochasticity is becoming increasingly essential in traffic flow research, given its notable influence in several applications, such as real-time traffic management. To consider stochasticity in macroscopic traffic flow modeling, this paper introduces a stochastic Lighthill-Whitham-Richards (SLWR) model, which not only captures equilibrium values in steady-state conditions but also describes stochastic variabilities. The SLWR model follows a conservation law, in which the free-flow speed is randomized to represent heterogeneities of drivers. To more accurately reflect real-life traffic patterns, a nonlinear speed-density relationship is considered. For addressing this highly nonlinear problem, a dynamically bi-orthogonal (DyBO) method is coupled with the Taylor series expansion technique. The results of simulation experiments show that the SLWR model can effectively describe the evolution of stochastic dynamic traffic with temporal or geometric bottlenecks. Moreover, the DyBO solutions exhibit reasonable accuracy while significantly reducing computation costs compared with the Monte Carlo method.

1. Introduction

Stochasticity, commonly observed in daily traffic, has increasingly become a focus in various traffic engineering applications, such as real-time traffic management. In traffic modeling, stochasticity introduces uncertainties and complexities to a system. For instance, the space-mean speed may vary in response to the mean density, even at the same location and traffic demand level from day to day. Compared to deterministic traffic flow models, stochastic traffic flow models can capture and convey more comprehensive information about traffic dynamics, which is necessary for advanced and precise traffic control and operation. However, stochastic traffic flow models may also increase computational burdens.

Macroscopic traffic flow models, which provide essential estimation of traffic states, need to be simple, robust, and efficiently solved for practical application. The classic Lighthill-Whitham-Richards

CONTACT Tianxiang Fan ✉ fantx@connect.hku.hk 🖃 Department of Civil Engineering, The University of Hong Kong, Hong Kong SAR, People's Republic of China; Jie Du ✉ jdu@math.ecnu.edu.cn 🖃 School of Mathematical Sciences, East China Normal University, Shanghai, People's Republic of China; Shanghai Key Laboratory of PMMP, East China Normal University, Shanghai, People's Republic of China; Key Laboratory of MEA (Ministry of Education), East China Normal University, Shanghai, People's Republic of China

Supplemental data for this article can be accessed http://doi.org/10.1080/21680566.2024.2419402.

(LWR) model (Lighthill and Whitham 1955; Richards 1956) is widely used due to its simplicity and ability to explain common traffic phenomena, such as shockwave propagation (Daganzo 1995; Jin 2012; 2013; Wong and Wong 2002; Zhang 2001). In physical terms, the LWR model captures kinematic shock and rarefaction waves in traffic flow, while in mathematical terms, it follows scalar hyperbolic conservation laws. However, the classic LWR model can only describe temporal means of traffic dynamics. Specifically, Prigogine and Herman (1971) highlighted the temporal mean dynamic characteristics of this model, and Jabari and Liu (2012) emphasized that traffic flow variables are defined as averages in the LWR model.

Incorporating stochasticity into the LWR model significantly increases computational burdens. The Monte Carlo (MC) method is widely used for solving stochastic problems. Although the MC model is robust, with its convergence rate independent of stochastic dimensionality, its convergence rate is limited (Cheng, Hou, and Zhang 2013a). To ensure applicability in engineering practice, efficient numerical solution methods must be identified. Compared to the Monte Carlo (MC) method, the dynamically bi-orthogonal (DyBO) method - one of the model reduction methods - exhibits high efficiency and sufficient accuracy. Fan et al. (2022) applied the DyBO method in cases involving linear speed-density relationships. However, when considering a nonlinear speed-density relationship, applying the DyBO method becomes challenging, as the expected value of stochastic exponential terms cannot be computed exactly in closed form.

To address the aforementioned research gaps in modeling and numerical methods, this paper aims to propose a Stochastic LWR (SLWR) model that incorporates a general nonlinear speed-density relationship and embeds a Taylor series expansion technique in the DyBO method for solving the resulting highly nonlinear problem.

The remainder of the paper is organized as follows: Section 2 reviews previous research on stochastic traffic flow modeling and numerical methods. Section 3 presents the general form of the SLWR model with a nonlinear speed-density relationship. Section 4 introduces the solution methods, specifically the formulation of the SLWR model with a general nonlinear speed-density relationship, involving DyBO equations and the Taylor series expansion technique. Section 5 details the numerical simulation experiments, in which the speed-density relationship is captured using Drake's model, and the traffic flow in temporal bottleneck and geometric bottleneck scenarios is simulated. Finally, Section 6 offers concluding remarks, emphasizing the contributions and limitations of this work.

2. Literature reivew

2.1. Stochastic traffic flow modeling

Traffic flow models are essential for describing and predicting traffic states and can be developed at different levels, from microscopic to macroscopic, for various purposes. Microscopic traffic flow models focus on individual vehicles and their interactions (Newell 1961), while macroscopic models treat traffic as a continuum. The classic LWR model (Lighthill and Whitham 1955; Richards 1956) is a first-order scalar hyperbolic equation, but it may not capture some typical traffic features, such as non-equilibrium traffic states in congested regimes. These limitations can be addressed by higher-order models, which consist of systems of hyperbolic equations. Lebacque, Mammar, and Haj-Salem (2007) developed a Generic Second Order Modeling (GSOM) family of traffic flow models, combining the LWR model with dynamics of driver-specific attributes. Additionally, Fan, Herty, and Seibold (2014) proposed a Generalized Aw-Rascle-Zhang model, which better reproduces the behavior of real data in fundamental diagrams in both free-flow and congested regimes. Although these deterministic models do not satisfy the need for considering stochasticity, they provide a solid foundation for developing stochastic traffic flow models.

In microscopic approaches, stochastic phenomena are reflected through the effects of anticipation, correlated vehicle motion across lanes, driving adaptation delays, or variations in safe time-gaps. Schreckenberg et al. (1995) investigated a probabilistic cellular automaton model, where

stochasticity was introduced as a probability of whether a vehicle may decrease its speed. In macroscopic approaches, one direct method of considering stochasticity is to include noise terms in the conservation laws (Gazis and Knapp 1971; Gazis and Liu 2003), fundamental diagrams (Ngoduy 2011; Li et al. 2012), or the cell transmission model (Boel and Mihaylova 2006). However, this can lead to negative densities and inconsistencies between mean dynamics and deterministic dynamics (Jabari and Liu 2012). To address these issues, Jabari and Liu (2012) devised a new stochastic traffic flow model, where the source of randomness is the uncertainty inherent in driver gap choice, represented by random vehicle time headways. Later, Jabari, Zheng, and Liu (2014) derived probabilistic macroscopic traffic flow relations from Newell's simplified car-following model, treating time headways and spacings as random variables. This model's probabilistic nature allows the effect of driver heterogeneity on the macroscopic relationships of traffic flow to be investigated. Martínez and Jin (2020) introduced heterogeneous (i.e. vehicle-dependent) jam densities to formulate a stochastic LWR model. This model, solved in Lagrangian coordinates, allows the effect of driver heterogeneity on the macroscopic relationships of traffic flow to be investigated both via simulations and analytically.

To better attribute physical meaning to the stochastic processes in traffic flow models, it is essential to investigate the sources of uncertainties. In some studies (Boel and Mihaylova 2006; Li et al. 2012), stochastic terms are treated as unknown factors without clear explanations. Previous research (Chen, Jia, and Varaiya 2001; Sumalee et al. 2011) has suggested that uncertainties may arise from exogenous sources, such as traffic states, road geometry, and weather conditions, as well as endogenous sources, like driving behaviors. Additionally, an empirical study by Cassidy and Windover (1995) demonstrated that driving behaviors may be influenced by drivers' memories or tendencies, which are consistent and difficult to alter. However, most stochastic traffic flow models assume that random effects occur at every time step, even when the step size is extremely small (Wang and Papageorgiou 2005; Li et al. 2012). Instead, Fan et al. (2022) developed a systematic model framework that allows stochasticity to reflect the diverse choices of different drivers while maintaining stability for each driver. Nevertheless, the authors utilized a linear speed-density relationship (Greenshields 1935). Although Greenshields' traffic stream model simplifies the relationship among traffic flow quantities and enables an easy exploration of the analytical properties of complex traffic models, field observations have indicated that the relationship between speed and density is generally nonlinear (Elefteriadou 2014).

2.2. Numerical methods

Stochasticity increases the complexity of traffic flow models, making it generally impossible to derive exact analytical solutions, particularly for highly nonlinear models. In such cases, numerical solutions are needed, which can significantly increase computational burdens, especially for stochastic problems. Although the Monte Carlo (MC) method can provide robust solutions, its low convergence rate is undesirable. To expedite convergence, several researchers have employed sampling methods. Caflisch (1998) introduced a quasi-MC method that used deterministic sequences instead of random or pseudo-random sequences. Giles (2008) proposed a multi-level MC method designed to reduce the computational complexity of estimating expected values for stochastic differential equations. Furthermore, Jahani et al. (2014) utilized an interval MC simulation in conjunction with an interval finite element method to evaluate failure probability in a structural reliability problem.

In addition to sampling methods, non-statistical methods have been explored. Xiu et al. (2002) introduced Wiener-Askey polynomial chaos to represent stochastic processes, thereby reducing dimensionality and leading to exponential convergence of the error. Wan and Karniadakis (2006) developed a multi-element generalized polynomial chaos approach to treat arbitrary probability measures for solving ordinary and partial differential equations with stochastic inputs. However, these methods are prone to the curse of dimensionality, where the basis terms of generalized polynomial chaos increase exponentially. Reduced-order models, such as proper orthogonal decomposition (Sirovich 1987) or Karhunen-Lòeve (KL) expansion (Newman 1996a; 1996b), can simplify the high-dimensional problem by using a low-dimensional structure to capture the original information. KL
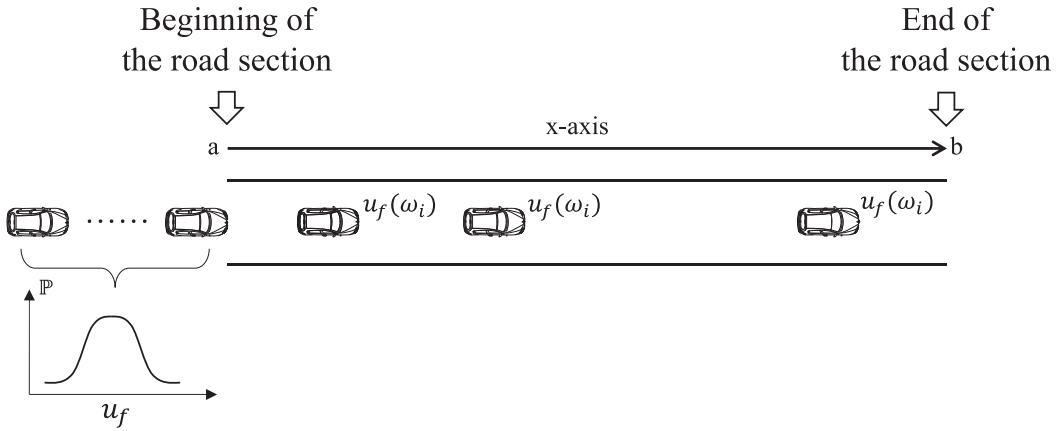
Figure 1. Conceptual diagram of the SLWR model.

expansion can provide the best basis for random fields as it optimizes the total mean squared error. However, it requires the construction of covariance matrices and solution of large-scale eigenvalue problems, which are computationally expensive tasks.

To address this limitation, researchers (Cheng, Hou, and Zhang 2013a; 2013b; Babaee et al. 2017; Choi, Sapsis, and Em 2014) have introduced approaches involving redundant representations with products of scalar, time-dependent, stochastic bases and deterministic, spatiotemporally depen- dent basis, such as dynamically orthogonal field equations or the dynamically bi-orthogonal (DyBO) method. The advantage of the DyBO method is that the process of learning the basis is offline, which reduces the time required to construct and solve the covariance matrix (Cheng, Hou, and Zhang 2013a; 2013b). However, this method remains to be applied in a macroscopic stochastic traf- fic flow model with a nonlinear fundamental relationship. Although Fan et al. (2022) demonstrated the efficacy of the DyBO method in cases involving linear speed-density relationships, its application to more general and realistic nonlinear relationships remains challenging. Therefore, in this paper, the SLWR model is extended to incorporate the general nonlinear speed-density relationship. The DyBO method, coupled with a Taylor series expansion technique, is used to solve the resulting highly nonlinear problem.

3. Model development

Figure 1 illustrates the concept of the SLWR model. This macroscopic model describes traffic flow as continuous fluid on a homogeneous road section. All vehicles enter the road section at the beginning and travel to the end, without any disturbance within the section. Each vehicle is characterized by distinct driving behaviors, which induce stochasticity.

To quantify the stochasticity, it is assumed to originate from heterogeneous drivers, with a driver's personality being consistent within a road section and reflected in their free-flow speeds. Moreover, it is assumed that these speeds, representing the desired speed choices on an empty or perceived empty road, can reflect such heterogeneities. These assumptions ensure that heterogeneous drivers exhibit different driving behaviors, and the behavior of a single driver is consistent along the road section. For example, aggressive drivers tend to drive faster than conservative drivers under the same traffic conditions, and these driver types do not abruptly change their behaviors.

Let u_f denote the free-flow speed, which is a random variable that follows an arbitrary distribution and is defined on a probability space $(\Omega, \mathcal{F}, \mathbb{P})$ to represent heterogeneous driving behaviors:

$$u_f : \Omega \to \mathbb{R}, \tag{1}$$

where Ω represents the sample space, $\mathcal{F}$ is a σ-algebra, $\mathbb{P}$ is a probability measure, and $\mathbb{R}$ is a real line. Then, $u_f(\omega)$ is the random free-flow speed that corresponds to the random event $\omega \in \Omega$.

At the beginning of the road section, the traffic flow is a stochastic process defined on the same probability space:

$$\{Q_{in}(t, \omega) : t \in [0, T], \omega \in \Omega\}, \tag{2}$$

where $Q_{in}(t, \omega)$ denotes the traffic flow at the beginning of the road section, and t represents the evolving time span from 0 to T. Therefore, every $t \in [0, T]$ corresponds to some random variable $Q_{in}(t, \cdot) : \Omega \to \mathbb{R}$, which indicates that the traffic flow at the beginning of the road section consists of heterogeneous drivers.

The traffic density, speed, and flow can be determined using fundamental diagrams. In this study, the general nonlinear relationship between speed and density is considered, which can be written in the form of the following definitional expression.

$$u(x, t, u_f(\omega)) = F(k(x, t, u_f(\omega))), F : [0, +\infty] \to [0, +\infty], F \in \mathcal{C}^\infty \tag{3}$$

$$q(x, t, u_f(\omega)) = k(x, t, u_f(\omega))F(k(x, t, u_f(\omega))) \tag{4}$$

where x represents the space domain, i.e. the length of the road section from point a to point b; $k(x, t, u_f(\omega))$ is the traffic density; $u(x, t, u_f(\omega))$ is the traffic speed; $q(x, t, u_f(\omega))$ is the traffic flow; and $F(\cdot)$ represents a differentiable and continuous function that describes the general nonlinear relationship between speed and density. Notably, the general nonlinear relationship between speed and density can be reflected by any traffic stream model, such as those of Greenberg, Underwood, Drakes, Pipes, and Newell, and the proposed SLWR model is equally applicable to all these traffic stream models.

By incorporating the stochastic free-flow speed into the conservation law, the generalized form of the SLWR model can be expressed as

$$\frac{\partial k(x, t, u_f(\omega))}{\partial t} + \frac{\partial q(x, t, u_f(\omega))}{\partial x} = 0, \quad x \in [a, b], t \in [0, T], \omega \in \Omega, \tag{5}$$

$$k(x, 0, u_f(\omega)) = k_0(x, u_f(\omega)), \tag{6}$$

$$q(a, t, u_f(\omega)) = Q_{in}(t, \omega), \tag{7}$$

where equation (5) represents the conservation law; and equations (6) and (7) represent the initial and boundary conditions, respectively.

Therefore, the proposed model indicates that the stochasticity, represented by the free-flow speed, is attributable to heterogeneous drivers. Furthermore, for a single sample, the free-flow speed remains constant throughout the period, ensuring the consistency of driving behavior. However, a challenge emerges when nonlinear functions are incorporated in the conservation law. Specifically, the use of such functions can make it difficult to calculate the expectation values if the DyBO method is attempted. In particular, this method expands the differential equation to polynomials, and with nonlinear functions, $E[F(k)] \neq F(\bar{k})$. To mitigate potential errors, the Taylor series expansion method is used to approximate the nonlinear function, and the convergence associated with different orders of expansion is evaluated.

4. Methodology

Because standard polynomial chaos expansion requires the construction of a covariance matrix at each time step, it is challenging to calculate the eigenvalues and eigenfunctions. In contrast, the DyBO method can construct spatial and stochastic bases that evolve orthogonally with time. In this section, the DyBO formulation of the SLWR model is derived. Once the SLWR model is transformed into a series

of deterministic partial differential equations (PDEs) and ordinary differential equations (ODEs), classic finite difference methods can be applied. The fifth-order weighted essentially non-oscillatory (WENO5) scheme is used in this study.

4.1. DyBO method

Denoting $\mathcal{L}$ as a differential operator and $\tilde{k}$ as a m-term truncated solution, the SLWR model can be represented as $\frac{\partial \tilde{k}}{\partial t} = \mathcal{L}\tilde{k} = -\frac{\partial \tilde{k}F(\tilde{k})}{\partial x}$. The solution $\tilde{k}$ can be described using the following equations:

$$\tilde{k}(x, t; \omega) = \bar{k}(x, t) + \boldsymbol{k}(x, t)\boldsymbol{Y}(\omega, t)^T, \tag{8}$$

$$\boldsymbol{k}(x, t) = (k_1(x, t), k_2(x, t), \ldots, k_m(x, t)), \quad m \in \mathbb{N}^+, \tag{9}$$

$$\boldsymbol{Y}(\omega, t) = (Y_1(\omega, t), Y_2(\omega, t), \ldots, Y_m(\omega, t)), \quad m \in \mathbb{N}^+, \tag{10}$$

where $\bar{k}$ is the mean; $\boldsymbol{k}$ is the spatial basis defined as a vector of eigenfunctions of the associated covariance function $Cov_k(x, y) = E[(k(x, t; \omega) - \bar{k}(x, t))(k(y, t; \omega) - \bar{k}(y, t))]$; and $\boldsymbol{Y}$ is the stochastic basis calculated as $Y_i(\omega, t) = \frac{1}{\lambda_i(t)} \int (k(x, t; \omega) - \bar{k}(x, t))k_i(x, t)dx, \ i = 1, 2, \cdots, m$.

The spatial and stochastic bases are orthogonal, satisfying the following conditions.

$$\left\langle \boldsymbol{k}^T, \boldsymbol{k} \right\rangle (t) = (\langle k_i, k_j \rangle) = (\lambda_i(t)\delta_{ij})_{m \times m}, \tag{11}$$

$$E[\boldsymbol{Y}^T\boldsymbol{Y}](t) = (E[Y_iY_j]) = \boldsymbol{I}, \tag{12}$$

where $\langle \cdot, \cdot \rangle$ is the inner product operator, e.g. $\langle k_i, k_j \rangle = \int k_ik_jdx$; $E[\cdot]$ is the expectation; λ_i denotes the eigenvalues of the covariance function $Cov_k(x, y)$; δ_{ij} is the Kronecker product; and $\boldsymbol{I}$ is the identity matrix.

Then, the DyBO formulation can be expressed as follows.

$$\frac{\partial \bar{k}}{\partial t} = E[\mathcal{L}\tilde{k}], \tag{13}$$

$$\frac{\partial \boldsymbol{k}}{\partial t} = -\boldsymbol{k}\boldsymbol{D}^T + E[\tilde{\mathcal{L}}\tilde{k}\boldsymbol{Y}], \tag{14}$$

$$\frac{d\boldsymbol{Y}}{dt} = -\boldsymbol{Y}\boldsymbol{C}^T + \left\langle \tilde{\mathcal{L}}\tilde{k}, \boldsymbol{k} \right\rangle \boldsymbol{\Lambda}_{\boldsymbol{k}}^{-1}, \tag{15}$$

where $\boldsymbol{C}$ and $\boldsymbol{D}$ are m-by-m matrices representing the projection coefficients of $\frac{\partial \boldsymbol{k}}{\partial t}$ and $\frac{d\boldsymbol{Y}}{dt}$ onto $\boldsymbol{k}$ and $\boldsymbol{Y}$, respectively; $\tilde{\mathcal{L}}\tilde{k} = \mathcal{L}\tilde{k} - E[\mathcal{L}\tilde{k}]$; and $\boldsymbol{\Lambda}_{\boldsymbol{k}}$ is the diagonal matrix of the tensor product of the spatial basis, i.e. $\boldsymbol{\Lambda}_{\boldsymbol{k}} = diag(\boldsymbol{k}^T, \boldsymbol{k})$.

The solutions of $\boldsymbol{C}$ and $\boldsymbol{D}$ are presented in an entry-wise manner:

$$C_{ii} = G_{*ii}, \tag{16}$$

$$C_{ij} = \frac{||k_j||^2}{||k_j||^2 - ||k_i||^2}(G_{*ij} + G_{*ji}), \text{ for } i \neq j, \tag{17}$$

$$D_{ii} = 0, \tag{18}$$

$$D_{ij} = \frac{1}{||k_j^2|| - ||k_i||^2}(||k_j||^2 G_{*ji} + ||k_i||^2 G_{*ij}), \text{ for } i \neq j, \tag{19}$$

$$\boldsymbol{G}_* = \boldsymbol{\Lambda}_{\boldsymbol{k}}^{-1} \left\langle \boldsymbol{k}^T, E[\tilde{\mathcal{L}}\tilde{k}\boldsymbol{Y}] \right\rangle, \tag{20}$$

where C_{ii} and C_{ij} are elements of matrix $\boldsymbol{C}$; D_{ii} and D_{ij} are elements of matrix $\boldsymbol{D}$; and G_{*ij} and G_{*ji} are elements of matrix $\boldsymbol{G}_*$.

As equations (13)–(15) still involve random variables, stochastic representations are needed. Hermite polynomials can be used because the random free-flow speed is assumed to follow a normal distribution. According to the Askey scheme (Xiu and Em 2003), Hermite polynomials can be defined as

$$H_n(x) = (-1)^n exp\left(\frac{x^2}{2}\right) \frac{d^n}{dx^n} exp(-x^2/2). \tag{21}$$

Here, $\boldsymbol{H} = (H_1, H_2, \cdots, H_{N_p}), N_p \in \mathbb{N}^+$ represents the N_p-term Hermite polynomials, which exclude the zero-index $\boldsymbol{H}_0 = 1$. Then,

$$\boldsymbol{Y} = \boldsymbol{HA}, \tag{22}$$

where $\boldsymbol{A}$ is an N_p-by-m matrix.

As the speed-density relationship is nonlinear, the Taylor series expansion is used in this study.

$$F(\tilde{k}) = \sum_{n=0}^{\infty} \frac{1}{n!} F^{(n)}(\bar{k})(\tilde{k} - \bar{k})^n = \sum_{n=0}^{\infty} \frac{1}{n!} F^{(n)}(\bar{k}) \boldsymbol{k} \boldsymbol{Y}^T \tag{23}$$

Then, the right-hand side of the SLWR model becomes

$$\mathcal{L}\tilde{k} = \frac{\partial(\bar{k} + \boldsymbol{HA}\boldsymbol{k}^T)}{\partial x} \sum_{n=0}^{\infty} \frac{1}{n!} F^{(n)}(\bar{k}) \boldsymbol{k} \boldsymbol{Y}^T + (\bar{k} + \boldsymbol{HA}\boldsymbol{k}^T) \frac{\partial \sum_{n=0}^{\infty} \frac{1}{n!} F^{(n)}(\bar{k}) \boldsymbol{k} \boldsymbol{Y}^T}{\partial x} \tag{24}$$

which is a linear combination.

This equation can be used to calculate the terms $E[\mathcal{L}\tilde{k}]$, $E[\tilde{\mathcal{L}\tilde{k}}\boldsymbol{H}]\boldsymbol{A} = E[(\mathcal{L}\tilde{k} - E[\mathcal{L}\tilde{k}])\boldsymbol{H}]\boldsymbol{A}$ and $E[\boldsymbol{H}^T \tilde{\mathcal{L}\tilde{k}}]$. Consequently, the DyBO formulation of the SLWR model can be re-written in terms of Hermite polynomials and Taylor series expansion:

$$\frac{\partial \bar{k}}{\partial t} = E[\mathcal{L}\tilde{k}] = \sum_{n=0}^{\infty} \frac{1}{n!} F^{(n)}(\bar{k}) \frac{\partial \boldsymbol{k}}{\partial x} \boldsymbol{k}^T + \frac{\partial \sum_{n=0}^{\infty} \frac{1}{n!} F^{(n)}(\bar{k}) \boldsymbol{k} \boldsymbol{k}^T}{\partial x}, \tag{25}$$

$$\frac{\partial \boldsymbol{k}}{\partial t} = -\boldsymbol{k}\boldsymbol{D}^T + E[\tilde{\mathcal{L}\tilde{k}}\boldsymbol{H}]\boldsymbol{A} = \boldsymbol{k}\boldsymbol{D}^T + \sum_{n=0}^{\infty} \frac{1}{n!} F^{(n)}(\bar{k}) \left(\frac{\partial \bar{k}}{\partial x} \boldsymbol{k} + \frac{\partial \boldsymbol{k}}{\partial x} \boldsymbol{A}^T \boldsymbol{H}^T \boldsymbol{k} \boldsymbol{A}^T \boldsymbol{H}^T \boldsymbol{H}\boldsymbol{A}\right)$$

$$+ \frac{\partial \sum_{n=0}^{\infty} \frac{1}{n!} F^{(n)}(\bar{k})}{\partial x} (\bar{k}\boldsymbol{k} + \boldsymbol{HA}\boldsymbol{k}^T \boldsymbol{k} \boldsymbol{A}^T \boldsymbol{H}^T \boldsymbol{H}\boldsymbol{A}), \tag{26}$$

$$\frac{dA}{dt} = -\boldsymbol{A}\boldsymbol{C}^T + \left\langle E[\boldsymbol{H}^T \tilde{\mathcal{L}\tilde{k}}], \boldsymbol{k} \right\rangle \Lambda_k^{-1}$$

$$= -\boldsymbol{A}\boldsymbol{C}^T + \left\langle \left(\sum_{n=0}^{\infty} \frac{1}{n!} F^{(n)}(\bar{k}) \left(\frac{\partial \bar{k}}{\partial x} \boldsymbol{A}\boldsymbol{k}^T + \boldsymbol{H}^T \boldsymbol{H}\boldsymbol{A} \frac{\partial \boldsymbol{k}^T}{\partial x} \boldsymbol{k} \boldsymbol{A}^T \boldsymbol{H}^T \right) \right.$$

$$\left. + \frac{\partial \sum_{n=0}^{\infty} \frac{1}{n!} F^{(n)}(\bar{k})}{\partial x} (\bar{k}\boldsymbol{A}\boldsymbol{k}^T + \boldsymbol{H}^T \boldsymbol{H}\boldsymbol{A}\boldsymbol{k}^T \boldsymbol{k} \boldsymbol{A}^T \boldsymbol{H}^T) \right), \boldsymbol{k} \right\rangle \Lambda_k^{-1}, \tag{27}$$

which yields the deterministic PDEs presented in equations (25) and (26) and ODE in equation (27).

4.2. WENO scheme

The WENO scheme, which use a nonlinear adaptive procedure to automatically select the locally smoothest stencil, is a high-order accurate finite difference method for problems with discontinuities in solutions (Xiong et al. 2011). Detailed derivation and applications can be found in the works of Shu

(2006; 2020). To account for possible shocks in the SLWR model, the WENO5 scheme is used in this study.

Given the space domain $[a, b]$ in the SLWR model, a uniform grid is used,

$$a = x_{\frac{1}{2}} < x_{\frac{3}{2}} < \cdots < x_{N-\frac{1}{2}} < x_{N+\frac{1}{2}} = b, \ N \in \mathbb{N}^+ \tag{28}$$

and the cells, cell centers, and cell size are defined as

$$I_i = \left[x_{i-\frac{1}{2}}, x_{i+\frac{1}{2}} \right], \ x_i = \frac{1}{2} \left(x_{i-\frac{1}{2}} + x_{i+\frac{1}{2}} \right), \ \Delta x = x_{i+\frac{1}{2}} - x_{i-\frac{1}{2}}, \ i = 1, 2, \cdots, N \tag{29}$$

Using mean values of the stochastic variable k, the DyBO formulation of the SLWR model can be expressed in the following form.

$$\frac{\partial \bar{k}}{\partial t} = -\frac{\partial f(\bar{k})}{\partial x}, \tag{30}$$

where $f(\bar{k})$ represents the right-hand-side of Equation (25).

This problem can be solved by using the following finite difference WENO method.

$$\frac{\partial \bar{k}_i}{\partial t} \approx -\frac{1}{\Delta x} \left(\hat{f}_{i+\frac{1}{2}} - \hat{f}_{i-\frac{1}{2}} \right), \tag{31}$$

where $\bar{k}_i$ is the approximation to the point value of $\bar{k}(x_i, t)$, and $\hat{f}_{i+\frac{1}{2}}$ and $\hat{f}_{i-\frac{1}{2}}$ represent numerical fluxes at nodes $x_{i+\frac{1}{2}}$ and $x_{i-\frac{1}{2}}$, respectively.

The numerical flux is a convex combination of reconstructed values $\hat{q}^{(r)}_{i+\frac{1}{2}}$ on the stencils.

$$\hat{f}_{i+\frac{1}{2}} = \sum_{r=0}^{2} \theta_r \hat{q}^{(r)}_{i+\frac{1}{2}}, \tag{32}$$

where θ_r are nonlinear weights.

The reconstructed values are obtained as

$$\hat{q}^{(r)}_{i+\frac{1}{2}} = \sum_{j=0}^{2} c_{rj} f_{i-r+j}, \quad r = 0, 1, 2. \tag{33}$$

The constants c_{rj} derived from the candidate stencils in Equation (34), are outlined in Table 1.

$$S_r(i) = \{ x_{i-r}, \ldots, x_{i-r+2} \}, \quad r = 0, 1, 2. \tag{34}$$

The nonlinear weights θ_r are defined as follows:

$$\theta_r = \frac{\tilde{\theta}_r}{\sum_{s=0}^{2} \tilde{\theta}_s}, r = 0, 1, 2 \tag{35}$$

Table 1. Constants c_{rj}.

r	$j = 0$	$j = 1$	$j = 2$
0	1/3	5/6	−1/6
1	−1/6	5/6	1/3
2	1/3	−7/6	11/6

with

$$\tilde{\theta}_r = \frac{\gamma_r}{(\varepsilon + \beta_r)^2}, \tag{36}$$

$$\gamma_0 = \frac{3}{10}, \ \gamma_1 = \frac{3}{5}, \ \gamma_2 = \frac{1}{10}, \tag{37}$$

$$\beta_0 = \frac{13}{12}(f_i - 2f_{i+1} + f_{i+2})^2 + \frac{1}{4}(3f_i - 4f_{i+1} + f_{i+2})^2, \tag{38}$$

$$\beta_1 = \frac{13}{12}(f_{i-1} - 2f_i + f_{j+1})^2 + \frac{1}{4}(f_{i-1} - f_{i+1})^2, \tag{39}$$

$$\beta_2 = \frac{13}{12}(f_{i-2} - 2f_{i-1} + f_i)^2 + \frac{1}{4}(f_{i-2} - 4f_{i-1} + 3f_i)^2. \tag{40}$$

where ε is set as 10^{-6} to prevent the denominator of $\tilde{\theta}_r$ being zero; γ_r represents the linear weights; and β_r denotes the smoothness indicators.

Note that the abovementioned equations exhibit an upwind bias in the optimal linear stencil. If the wind direction is reversed, the procedure results in a mirror image with respect to $x_{i+1/2}$. To address the potential changes in wind direction, a more robust approach is to use global flux splitting. To this end, the Lax-Friedrichs splitting method is used herein.

$$f(\bar{k}) = f^+(\bar{k}) + f^-(\bar{k}), \tag{41}$$

$$f^\pm(\bar{k}) = \frac{1}{2}(f(\bar{k}) \pm \alpha\bar{k}), \tag{42}$$

$$\alpha = max_{\bar{k}}|f'(\bar{k})|, \tag{43}$$

where $f^+(\bar{k})$ and $f^-(\bar{k})$ are the splitting fluxes for the upwind and downwind directions, respectively.

The WENO approximation of $\mathcal{L}(k)$ is represented as $\mathcal{L}(\bar{k}) = -\frac{1}{\Delta x}\left(\hat{f}_{i+\frac{1}{2}} - \hat{f}_{i-\frac{1}{2}}\right)$, and then, equation (30) can be re-written as

$$\frac{\partial \bar{k}}{\partial t} = \mathcal{L}(\bar{k}). \tag{44}$$

The above equation can be solved by using the third-order total variation diminishing Runge-Kutta method. Further, the temporal domain $[0, T]$ is divided into several discrete time points $0 = t_0 < t_1 < \cdots < t_{N_t} = T$, and denote the numerical approximation to $\bar{k}$ at the nth time step t_n as $\bar{k}^n$. First, $\bar{k}^0$ can be obtained with the initial condition. Then, starting from the known value $\bar{k}^n (n \in \mathbb{N})$ at the nth time step t_n, the value $\bar{k}^{n+1}$ at the next time step t_{n+1} can be computed by using the following equations.

$$\bar{k}^{(1)} = \bar{k}^n + \Delta t \mathcal{L}(\bar{k}^n), \tag{45}$$

$$\bar{k}^{(2)} = \frac{3}{4}\bar{k}^n + \frac{1}{4}(\bar{k}^{(1)} + \Delta t \mathcal{L}(\bar{k}^{(1)})), \tag{46}$$

$$\bar{k}^{n+1} = \frac{1}{3}\bar{k}^n + \frac{2}{3}(\bar{k}^{(2)} + \Delta t \mathcal{L}(\bar{k}^{(2)})), \tag{47}$$

where $\Delta t = t_{n+1} - t_n$ is the time step size, and $\bar{k}^{(1)}$ and $\bar{k}^{(2)}$ are the intermediate stages.

5. Numerical examples

To demonstrate the physical properties of the SLWR model, two simulation experiments are conducted: one involving a temporal bottleneck due to lane blockage and the other including a geometric bottleneck due to road characteristics, using the DyBO method and MC method. The MC results are used as a benchmark to validate the accuracy of the DyBO method. Various terms of spatial and Hermite polynomial bases are evaluated in the sensitivity analysis.

5.1. Nonlinear speed-density relationship

In this example, Drake's model is used to describe the nonlinear fundamental relationship between the traffic density and speed. Using the definitional relationship, the traffic flow can be obtained.

$$u(x, t, u_f(\omega)) = u_f(\omega)exp\left(-\left(\frac{k(x, t, u_f(\omega))}{k_o}\right)^2/2\right) \tag{48}$$

$$q(x, t, u_f(\omega)) = k(x, t, u_f(\omega))u(x, t, u_f(\omega)), \tag{49}$$

where k_o is the optimal density, set as a constant value of 50 veh/km in this paper.

Using equations (47) and (48), stochastic patterns of the fundamental diagrams can be derived, as shown in Figure 2, corresponding to the stochastic patterns of the fundamental relationship.

Further, the free-flow speed is interpreted as an inherent inclination of a driver to select a speed under free-flow conditions, and when this speed is randomized, it can be concluded that that the corresponding traffic flow and time headway also become random variables, as illustrated below.

$$E(q) = \bar{u}_f kexp(-k^2/2k_o^2), \tag{50}$$

$$Var(q) = \sigma_{uf}^2 k^2 exp(-k^2/k_o^2), \tag{51}$$

$$E(\tau) = \frac{1}{\bar{u}_f k}exp(k^2/2k_o^2) + \frac{1}{\bar{u}_f^3 k}\sigma_{uf}^2 exp(k^2/2k_o^2), \tag{52}$$

$$Var(\tau) = \frac{1}{\bar{u}_f^4 k^2}\sigma_{uf}^2 exp(k^2/k_o^2) - \frac{1}{\bar{u}_f^6 k^2}\sigma_{uf}^4 exp(k^2/k_o^2), \tag{53}$$

where $E(q)$ is the mean of traffic flow, $Var(q)$ is the variance of traffic flow, $E(\tau)$ is the mean of time headway, $Var(\tau)$ is the variance of time headway, $\bar{u}_f$ is the mean of free-flow speed, and $\sigma_{u_f}^2$ is the variance of free-flow speed.

Incorporating equations (47) and (48), the governing equation of the SLWR model can be written as

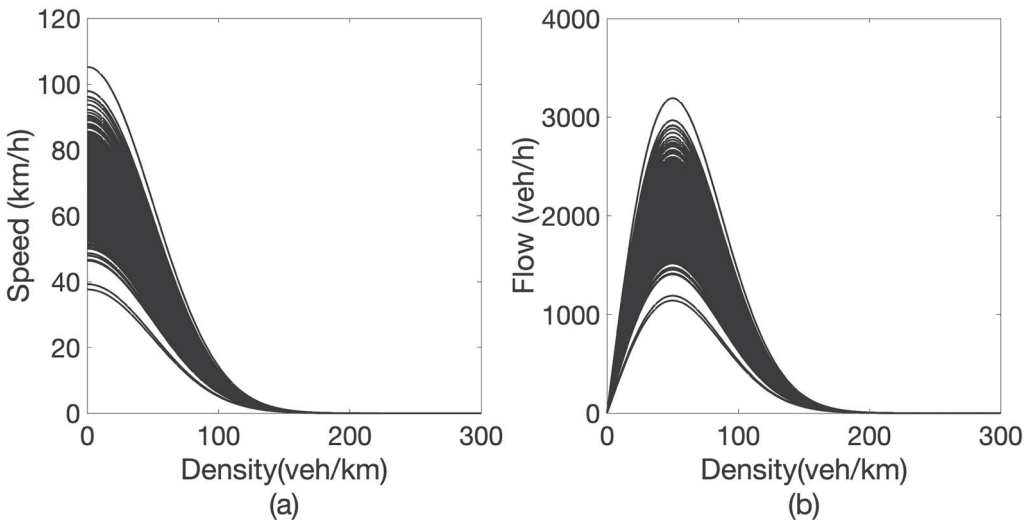$$\frac{\partial k(x, t, u_f(\omega))}{\partial t} = \mathcal{L}k$$

Figure 2. Stochastic fundamental diagram.

$$= \left(\frac{k(x, t, u_f(\omega))^2}{k_o^2} - 1 \right) u_f(\omega) exp \left(\frac{-k(x, t, u_f(\omega))^2}{2k_o^2} \right) \frac{\partial k(x, t, u_f(\omega))}{\partial x}. \tag{54}$$

Using the m-term truncated solution $\tilde{k}$, the following expression can be obtained:

$$\mathcal{L}\tilde{k} = \left(\frac{(\bar{k} + \mathbf{k}\mathbf{Y}^T)^2}{k_o^2} - 1 \right) u_f(\omega) exp \left(\frac{-(\bar{k} + \mathbf{k}\mathbf{Y}^T)^2}{2k_o^2} \right) \frac{\partial (\bar{k} + \mathbf{k}\mathbf{Y}^T)}{\partial x}. \tag{55}$$

Because this equation involves an exponential term, the standard derivation procedure of the DyBO method cannot be directly applied. To address this problem, a Taylor series expansion is used:

$$f(\tilde{k}) = exp \left(-\frac{\tilde{k}^2}{2k_o^2} \right) = f(\bar{\bar{k}}) + f'(\bar{\bar{k}})(\tilde{k} - \bar{\bar{k}}) + \frac{1}{2}f''(\bar{\bar{k}})(\tilde{k} - \bar{\bar{k}})^2 + O(\Delta x^2), \tag{56}$$

where

$$f'(\tilde{k}) = -\frac{\tilde{k}}{k_o^2} exp \left(-\frac{\tilde{k}^2}{2k_o^2} \right), \tag{57}$$

$$f''(\tilde{k}) = -\frac{1}{k_o^2} exp \left(-\frac{\tilde{k}^2}{2k_o^2} \right) + \frac{\tilde{k}^2}{k_o^4} exp \left(-\frac{\tilde{k}^2}{2k_o^2} \right). \tag{58}$$

Then, the exponential term can be approximated as follows.

$$exp \left(-\frac{\tilde{k}^2}{2k_o^2} \right) = exp \left(-\frac{\bar{k}^2}{2k_o^2} \right) - \frac{\bar{k}}{k_o^2} exp \left(-\frac{\bar{k}^2}{2k_o^2} \right) \mathbf{H}\mathbf{A}\mathbf{k}^T$$

$$+ \frac{1}{2} \left(-\frac{1}{k_o^2} exp \left(-\frac{\bar{k}^2}{2k_o^2} \right) + \frac{\bar{k}^2}{k_o^4} exp \left(-\frac{\bar{k}^2}{2k_o^2} \right) \right) \mathbf{k}\mathbf{A}^T\mathbf{H}^T\mathbf{H}\mathbf{A}\mathbf{k}^T. \tag{59}$$

As the free-flow speed is a random parameter, it must be represented using Hermite polynomials. Here, $Z_{u_f} = \mathbf{c}\mathbf{H}^T$ denotes a standard normal (i.e. $Z_{u_f} \sim N(0,1)$),) where $\mathbf{c} = (1, 0, \cdots, 0)$ represents the expansion constants:

$$u_f(\omega) = \overline{u_f} + \sigma_{u_f}\mathbf{c}\mathbf{H}^T, \tag{60}$$

where $\overline{u_f}$ is the mean, and σ_{u_f} is the standard deviation of the random free-flow speed.

Through simple calculations, the following expression can be obtained:

$$\mathcal{L}\tilde{k} = \left(\frac{\bar{k}^2 + 2\bar{k}\mathbf{H}\mathbf{A}\mathbf{k}^T + \mathbf{k}\mathbf{A}^T\mathbf{H}^T\mathbf{H}\mathbf{A}\mathbf{k}^T}{k_o^2} - 1 \right) [\overline{u_f} + \sigma_{u_f}\mathbf{c}\mathbf{H}^T]$$

$$\times \left[exp \left(-\frac{\bar{k}^2}{2k_o^2} \right) - \frac{\bar{k}}{k_o^2} exp \left(-\frac{\bar{k}^2}{2k_o^2} \right) \mathbf{H}\mathbf{A}\mathbf{k}^T + \frac{1}{2} \left(-\frac{1}{k_o^2} exp \left(-\frac{\bar{k}^2}{2k_o^2} \right) \right. \right.$$

$$\left. \left. + \frac{\bar{k}^2}{k_o^4} exp \left(-\frac{\bar{k}^2}{2k_o^2} \right) \right) \mathbf{k}\mathbf{A}^T\mathbf{H}^T\mathbf{H}\mathbf{A}\mathbf{k}^T \right] \left(\frac{\partial \bar{k}}{\partial x} + \mathbf{H}\mathbf{A} \frac{\partial \mathbf{k}^T}{\partial x} \right) \tag{61}$$

Subsequently, the following terms $E[\mathcal{L}\tilde{k}]$, $E[\mathcal{L}\tilde{k}\mathbf{H}]\mathbf{A} = E[(\mathcal{L}\tilde{k} - E[\mathcal{L}\tilde{k}])\mathbf{H}]\mathbf{A}$, $E[\mathbf{H}^T\mathcal{L}\tilde{k}]$ can be easily calculated as the embedded Taylor series expansion transforms them into linear combinations. Thus, the DyBO formulation of the SLWR model can be obtained using equations (25)–(27). Explicit terms are presented in the Appendix B.

5.2. Example 1

5.2.1. Settings

Consider a 2-km-long segment of a geometrically homogeneous highway road. There are no entrances or exits in the middle of this road. The random free-flow speed follows a normal distribution with a mean of 70 km/h and standard deviation of 10 km/h, i.e. $u_f \sim N(70, 100)$. Moreover, the optimal density is a constant, i.e. $k_o = 50\ veh/km$. Initially, the road is empty, and the left boundary involves a trapezoidal traffic flow over time, as shown in Figure 3.

To examine the discontinuities of the solutions, a traffic incident is assumed to occur at the end of the road section, blocking the whole traffic from t = 0.75 h to t = 0.77 h. During this period, no vehicles can leave the road section, and thus, a queue emerges and propagates upstream. After this period, the queue starts to dissipate.

5.2.2. Numerical results

A warm-up simulation with the MC method is conducted for a short period of 5 min to obtain initial values of the spatial and stochastic bases. Subsequently, the DyBO formulation is implemented, which allows the spatial and stochastic bases to evolve over time while remaining dynamically bi-orthogonal. This approach eliminates the costs associated with the generation of covariance matrices and solution of eigen-problems. Figure 4 shows the evolving patterns of the spatial and stochastic bases. Significantly variability of the stochastic basis is observed at t = 0.77 h, indicating abrupt change in the traffic density due to the queue propagation arising from the blockage. This observation highlights that the DyBO formulation of the spatial and stochastic bases can capture the variability of the randomness in the SLWR model.

Given the highly nonlinear nature of the SLWR model, obtaining analytical solutions is typically impractical. In contrast, the MC method is robust and can converge to the expected value with large sample sizes due to the law of large numbers. By conducting simulations with different sample sizes, 12,800 MC samples are selected as a benchmark in this study. The relative root-mean-squared error
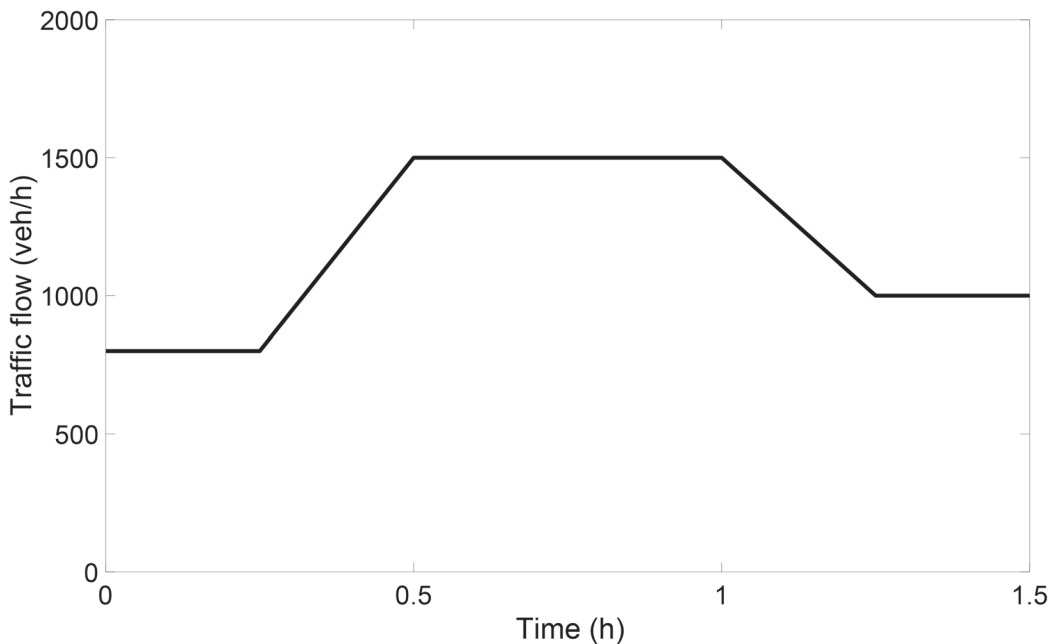

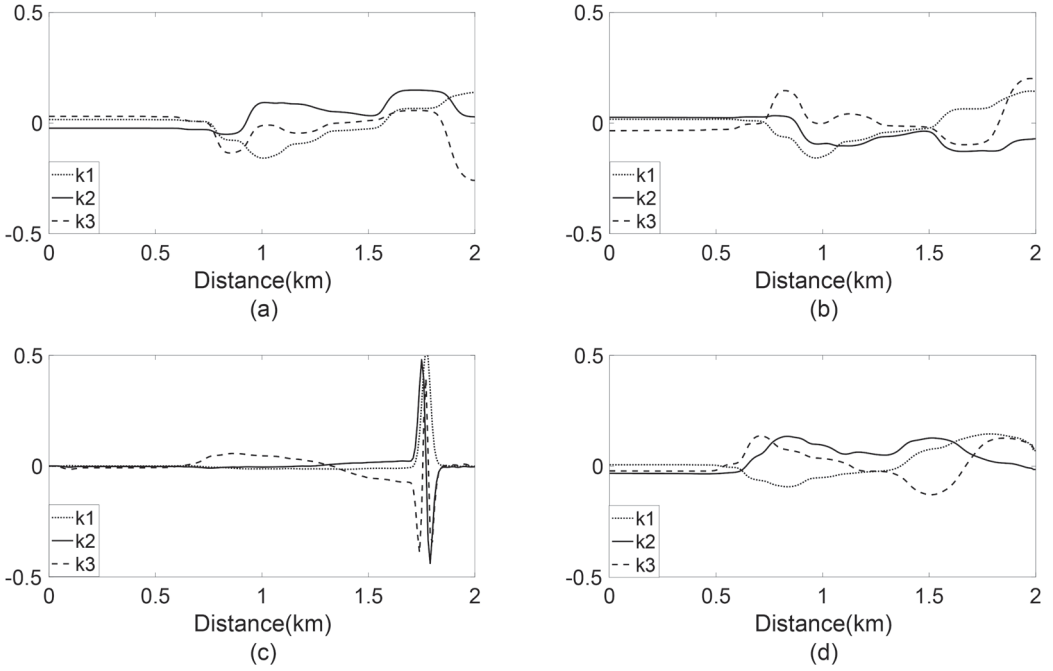**Figure 3.** Upstream demand.

Figure 4. Spatial basis at different times: (a) 0.083 h; (b) 0.3 h; (c) 0.77 h; (d) 1.2 h.

(RRMSE) is defined to compare the accuracy of the DyBO solutions with against the benchmark MC results.

$$RRMSE_\rho = \frac{\sqrt{\frac{1}{N}\sum_{it}\left(\rho_{it}^{(k)} - \rho_{it}^*\right)^2}}{\frac{1}{N}\sum_{it}\rho_{it}^*} \times 100\%, \quad RRMSE_\sigma = \frac{\sqrt{\frac{1}{N}\sum_{it}\left(\sigma_{it}^{(k)} - \sigma_{it}^*\right)^2}}{\frac{1}{N}\sum_{it}\sigma_{it}^*} \times 100\%, \quad (62)$$

where $\rho_{it}^{(k)}$ and $\sigma_{it}^{(k)}$ are the mean (MEAN) and standard deviation (SDEV) of the density of the *kth* case for grid point (i, t), respectively; ρ_{it}^* and σ_{it}^* are the converged MEAN and SDEV of the density from the MC scheme, respectively; and N is the total number of grid points (space and time).

The accuracy of the DyBO method is affected by the truncated terms. Achieving a balance between complexity and accuracy is essential. Through a comparison with the benchmark results obtained using the MC method, different numbers of spatial basis ($m = 3, 7, 11, 15, 19$) and Hermite polynomials ($N_p = 4, 8, 12$) are used to calculate the MEAN and SDEV values, as shown in Table 2. The RRMSEs of both MEAN and SDEV decrease with increases in the numbers of terms of the spatial basis and Hermite polynomials. In addition, the computation time is substantially reduced compared with the benchmark solution of the MC method, which requires more than 3,500 min. When $N_p = 12$ and $m = 19$, the RRMSEs of the MEAN and SDEV are below 2% and 5%, which may be considered acceptable. For this example, it is observed that the DyBO solutions effectively converge to the benchmark results with increasing numbers of terms of the spatial basis and Hermite polynomials.

Three representative time slots are selected to demonstrate the evolution patterns of the SLWR models. Before the incident occurs, vehicles enter from the beginning of the road section and travel to the end without any disturbance. Figure 5 illustrates the density patterns at t = 0.3 h. The density MEAN evolves smoothly along the road section, with a staircase-like fluctuation downstream. This phenomenon occurs because heterogeneous drivers drive at different speeds, with faster drivers covering more distance within the same time slot. In addition, with increasing numbers of terms of the spatial

Table 2. RRMSEs of statistical quantities computed by the DyBO and MC methods.

	No. of Hermite polynomials								
	$N_p = 4$			$N_p = 8$			$N_p = 12$		
No. of spatial basis terms, m	MEAN	SDEV	Time (min)	MEAN	SDEV	Time (min)	MEAN	SDEV	Time (min)
3	21.1%	38.1%	2.26	16.6%	33.6%	2.32	13.9%	29.9%	2.41
7	6.6%	19.3%	2.40	5.2%	9.9%	2.50	4.3%	8.5%	2.59
11	5.0%	14.3%	2.58	2.9%	7.3%	2.69	2.6%	5.2%	2.74
15	3.5%	13.8%	2.70	2.3%	5.9%	2.88	1.7%	5.0%	2.95
19	2.6%	13.0%	2.82	1.7%	5.3%	3.12	1.6%	5.0%	3.17
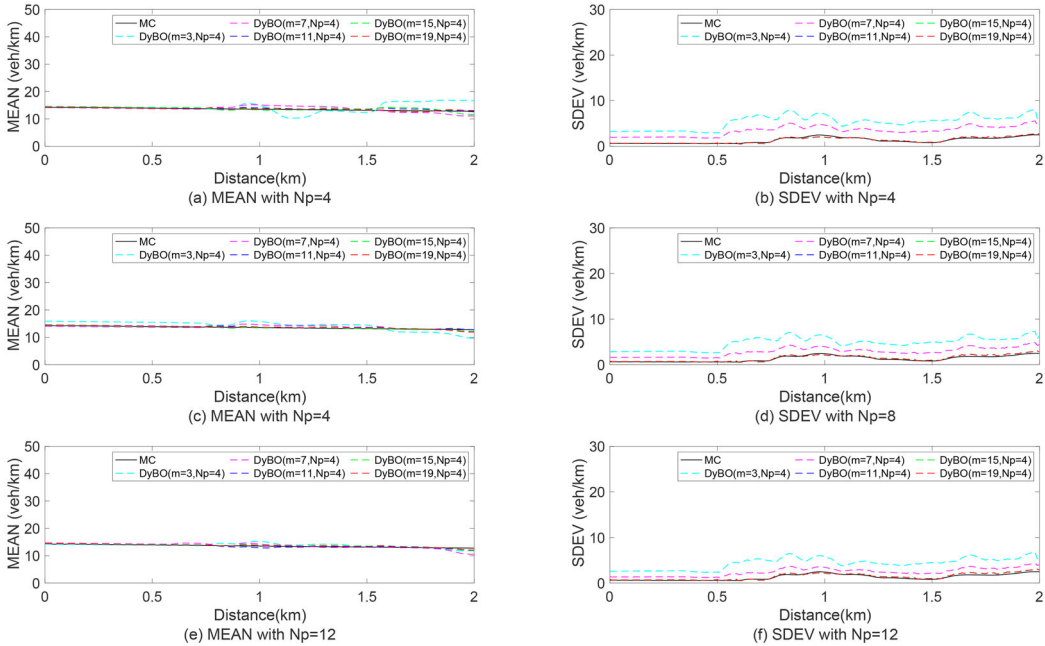
Figure 5. Density patterns at t $=$ 0.3 h.

basis and Hermite polynomials, the MEAN and SDEV values approach the benchmark results of the MC method.

When the incident occurs at the end of the road section, preventing vehicles from exiting while upstream vehicles continuously arrive, a queue forms. Figure 6 shows the density patterns at $t = 0.78$ h. A backward shock wave can be observed in the MEAN of the density. Furthermore, the SDEV of the density remains low and stable before the shock wave, surges and becomes unstable in the region in which the MEAN dramatically increases, and then stabilizes to a low value as the MEAN gradually peaks. This pattern indicates that heterogeneous drivers may arrive at the starting point of the queue at different times, leading to significant variations in the densities. The speed differences among vehicles diminish when the traffic approaches a fully congested state. The SDEV is expected to increase with a larger number of heterogeneous drivers. Although the incident introduces a discontinuity, the DyBO solutions exhibit strong convergence to the benchmark result, and the accuracy can be increased by adding more spatial terms and Hermite polynomials.

After the incident is resolved, vehicles can leave the road section, and thus, the queue begins to disperse. Figure 7 shows the density patterns at t $=$ 1.2 h. There is no traffic congestion at this point, and the MEAN and SDEV remain stable along the road section, albeit slightly larger than those at t $=$ 0.3
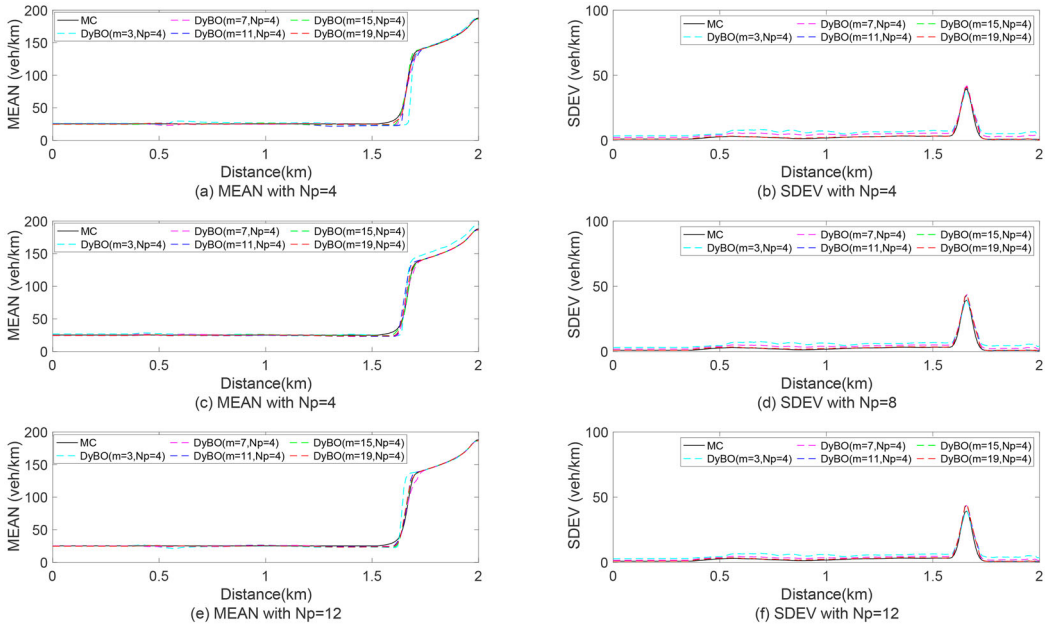
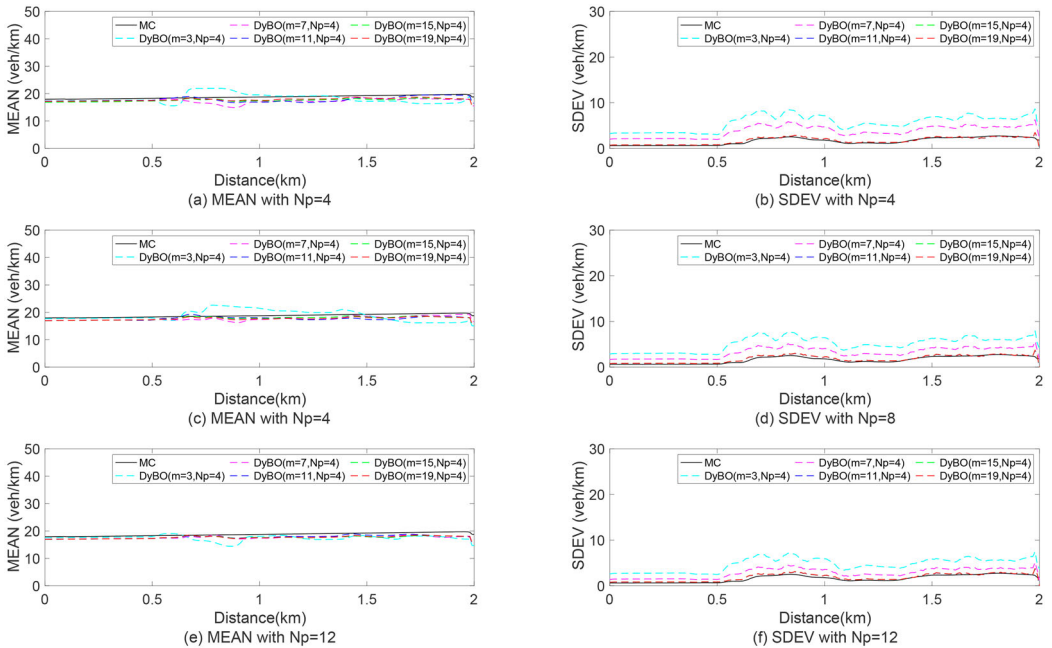**Figure 6.** Density patterns at t = 0.78 h.

Figure 7. Density patterns at t = 1.2 h.

h due to more vehicles entering from the beginning of the road section. These trends show that the proposed model and solution method can accommodate different boundary conditions.

Because Taylor series expansion is applied to approximate the exponential terms in the DyBO formulation, it is necessary to examine its effects on errors. Figure 8 shows the RRMSEs of MEAN and
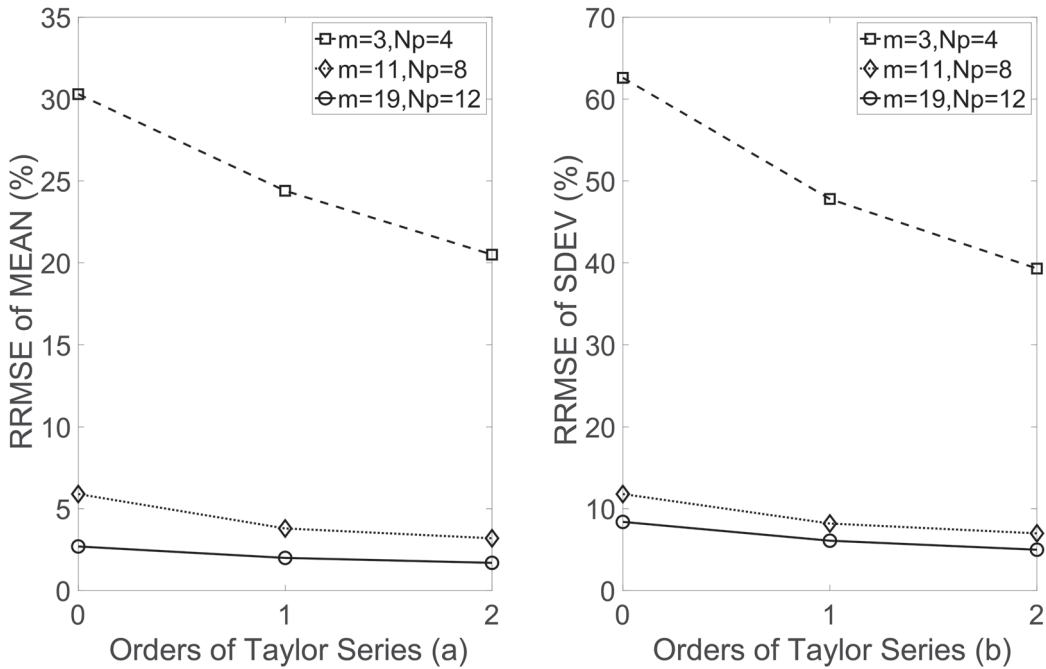
Figure 8. RRMSE with different orders of Taylor series expansion: (a) MEAN; (b) SDEV.

Table 3. Optimal densities of different road sections.

Road section	Length (km)	Optimal density (veh/km)	Description
1	0–3	50	Adequately long to hold queuing vehicles
2	3–4	35	Decrease in capacity
3	4–5	50	Same setting as that of road section 1
4	5–6	30	Second bottleneck with further decrease in capacity to demonstrate the second queue at the downstream end

SDEV for different orders of Taylor series expansion. Three cases ($m = 3$, $N_p = 4$; $m = 11$, $N_p = 8$; $m = 19$, $N_p = 12$) are considered, and the results show that the accuracy is enhanced with an increase in the order of Taylor series expansion.

5.3. Example 2

5.3.1. Settings

As shown in Table 3, this example features a 6-km-long highway with varying road characteristics, divided by two geometric bottlenecks. The optimal density represents these heterogeneous conditions. Road sections with different optimal densities have various capacities, potentially resulting in queuing at the upstream end when the capacity of the downstream section is exceeded. Other settings are the same as those in the first example, except for the extended 2-h simulation period, implemented to observe queue dissipation at the downstream end.

5.3.2. Numerical results

To demonstrate shock propagations between different road sections, DyBO solutions with 11 spatial basis terms and 8 Hermite polynomial terms and MC solutions with 1,000 MC samples are obtained. Road sections 2 and 4 have lower optimal densities and thus lower capacities. As the traffic demand
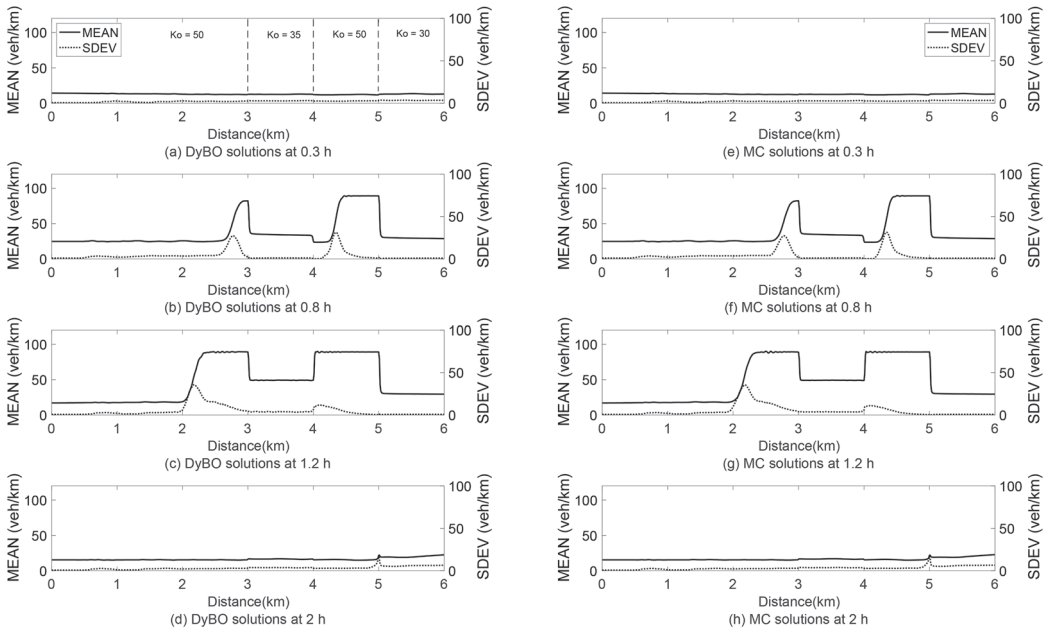
Figure 9. Density patterns with geometric bottlenecks.

exceeds these capacities, queues form, as expected. In the absence of any blockage at the end of the road section, the queues are expected to gradually dissipate and eventually clear if the traffic demand remains below capacity. Typical time slots are selected to demonstrate density evolution along this heterogeneous highway.

As shown in Figure 9, at $t = 0.3$ h, the traffic demand is lower than the capacities of all road sections, and thus, no queue is formed. However, the MEAN values for road sections 2 and 4 are slightly higher than those for road sections 1 and 3, owing to their lower optimal densities. At $t = 0.8$ h, two queues form at the beginning of road sections 2 and 4. These queues propagate upstream because the traffic demand exceeds the capacities of road sections 2 and 4. The MEAN value for the downstream queues is slightly higher than that of the upstream queues owing to the lower optimal density of the former. The two queues dissipate upon reaching their optimal densities (i.e. 35 and 30 veh/km, respectively). When the traffic demand exceeds capacities of the bottlenecks, the queues continue to grow. At $t = 1.2$ h, the MEAN value of road section 2 exceeds 35 veh/km (i.e. the optimal density), indicating congestion. The downstream queue overflows into road section 2. When the traffic demand is lower than the capacities of the bottlenecks, the queue begins to dissipate. At $t = 2$ h, the queue is cleared. These density patterns demonstrate the effectiveness of the DyBO method in solving the SLWR model with geometric bottlenecks.

6. Conclusions

This study was aimed at extending the applicability of the SLWR model from linear speed-density relationships to nonlinear speed-density relationships, which can better reflect real-world traffic streams. Compared with the linear speed-density relationship explored in a recent study(Fan et al. 2022), this nonlinear extension increases the model complexity, rendering the previous DyBO formulation inapplicable. The challenge associated with considering the nonlinear speed-density relationship is that expectations of the nonlinear terms cannot be directly calculated during the DyBO formulation. Taylor

series expansion represents a promising strategy to approximate the nonlinear terms, and acceptable accuracy can be achieved when sufficiently high orders are used. Simulation experiments were conducted using Drake's model, in which the free-flow speed was treated as a random variable. The numerical results demonstrated stochastic variabilities along the road section over time. Moreover, typical phenomena, such as queuing and shock propagations, in the presence of temporal or geometric bottlenecks could be simulated.

Compared with the MC method, the DyBO method requires considerably less computation time while maintaining reasonable accuracy, and thus, it is more applicable in engineering practice. For instance, in highway design, the proposed model can help identify critical locations resulting from varying user distributions on different days. There might be situations where the average density at specific locations is moderate, but with a large variance, leading to exceptional congestion on crucial days that could be overlooked during the standard design process based on average user characteristics. Furthermore, the likelihood of such critical situations can be quantified, allowing for a trade-off between operational performance and construction cost. Another application can be related to road network design. Traditional methods require updating the evaluation models each time network conditions change. Incorporating stochastic factors in these cases would lead to significant computational costs. In such scenarios, the DyBO method can considerably reduce the computational burden. However, real-world scenarios may have multiple sources of stochasticity. Future research can be aimed at extending the proposed framework to consider different traffic stream models and multiple random parameters.

Disclosure statement

Funding

References

Babaee, H., M. Choi, T. P. Sapsis, and G. E. Karniadakis. 2017. "A Robust Bi-Orthogonal/Dynamically-Orthogonal Method Using the Covariance Pseudo-Inverse with Application to Stochastic Flow Problems." *Journal of Computational Physics* 344: 303–319.
Boel, R., and L. Mihaylova. 2006. "A Compositional Stochastic Model for Real Time Freeway Traffic Simulation." *Transportation Research Part B: Methodological* 40 (4): 319–334.
Caflisch, R. E. 1998. "Monte Carlo and Quasi-Monte Carlo Methods." *Acta Numerica* 7: 1–49.
Cassidy, M. J., and J. R. Windover. 1995. "Methodology for Assessing Dynamics of Freeway Traffic Flow." *Transportation Research Record* 1484: 73–79.
Chen, C., Z. Jia, and P. Varaiya. 2001. "Causes and Cures of Highway Congestion." *IEEE Control Systems Magazine* 21 (6): 26–33.
Cheng, M., T. Y. Hou, and Z. Zhang. 2013a. "A Dynamically Bi-Orthogonal Method for Time-Dependent Stochastic Partial Differential Equations I: Derivation and Algorithms." *Journal of Computational Physics* 242: 843–868.
Cheng, M., T. Y. Hou, and Z. Zhang. 2013b. "A Dynamically Bi-Orthogonal Method for Time-Dependent Stochastic Partial Differential Equations II: Adaptivity and Generalizations." *Journal of Computational Physics* 242: 753–776.
Choi, M., T. P. Sapsis, and K. G. Em. 2014. "On the Equivalence of Dynamically Orthogonal and Bi-Orthogonal Methods: Theory and Numerical Simulations." *Journal of Computational Physics* 270: 1–20.
Daganzo, C. F. 1995. "Requiem for Second-Order Fluid Approximations of Traffic Flow." *Transportation Research Part B: Methodological* 29 (4): 277–286.
Elefteriadou, L. 2014. *An Introduction to Traffic Flow Theory*. New York: Springer.
Fan, S., M. Herty, and B. Seibold. 2014. "Comparative Model Accuracy of a Data-Fitted Generalized Aw-Rascle-Zhang Model." *Networks and Heterogeneous Media* 9 (2): 239–268.

Fan, T., S. C. Wong, Z. Zhang, and J. Du. 2022. "A Dynamically Bi-Orthogonal Solution Method for a Stochastic Lighthill-Whitham-Richards Traffic Flow Model." *Computer-Aided Civil and Infrastructure Engineering* 38: 1447–1461.

Gazis, Denos C., and Charles H. Knapp. 1971. "On-Line Estimation of Traffic Densities from Time-Series of Flow and Speed Data." *Transportation Science* 5 (3): 283–301.

Gazis, Denos, and Chiu Liu. 2003. "Kalman Filtering Estimation of Traffic Counts for Two Network Links in Tandem." *Transportation Research Part B: Methodological* 37 (8): 737–745.

Giles, M. B. 2008. "Multilevel Monte Carlo Path Simulation." *Operations Research* 56 (3): 607–617.

Greenshields, B. D. 1935. "A Study of Traffic Capacity." *Proceedings of the Highway Research Record* 10: 448–477.

Jabari, S. E., and H. X. Liu. 2012. "A Stochastic Model of Traffic Flow: Theoretical Foundations." *Transportation Research Part B: Methodological* 46 (1): 156–174.

Jabari, Saif Eddin, Jianfeng Zheng, and Henry X. Liu. 2014. "A Probabilistic Stationary Speed-Density Relation Based on Newell's Simplified Car-Following Model." *Transportation Research Part B: Methodological* 68: 205–223.

Jahani, E., R. L. Muhanna, M. A. Shayanfar, and M. A. Barkhordari. 2014. "Reliability Assessment with Fuzzy Random Variables Using Interval Monte Carlo Simulation." *Computer-Aided Civil and Infrastructure Engineering* 29 (3): 208–220.

Jin, W. L. 2012. "A Kinematic Wave Theory of Multi-Commodity Network Traffic Flow." *Transportation Research Part B: Methodological* 46 (8): 1000–1022.

Jin, W. L. 2013. "A Multi-Commodity Lighthill-Whitham-Richards Model of Lane-Changing Traffic Flow." *Transportation Research Part B: Methodological* 57: 361–377.

Lebacque, J.-P., S. Mammar, and H. Haj-Salem. 2007. "Generic Second Order Traffic Flow Modelling." *Transportation and Traffic Theory* 2007: 755–776.

Li, J., Q. Y. Chen, H. Wang, and D. Ni. 2012. "Analysis of LWR Model with Fundamental Diagram Subject to Uncertainties." *Transportmetrica* 8 (6): 387–405.

Lighthill, M. J., and G. B. Whitham. 1955. "On Kinematic Waves. II. A Theory of Traffic Flow on Long Crowded Roads." *Proceedings of the Royal Society of London. Series A, Mathematical and Physical Sciences* 229 (1178): 317–345.

Martínez, Irene, and Wen Long Jin. 2020. "Stochastic LWR Model with Heterogeneous Vehicles: Theory and Application for Autonomous Vehicles." *Transportation Research Procedia* 47: 155–162.

Newell, G. F. 1961. "Nonlinear Effects in the Dynamics of car Following." *Operations Research* 9: 209–229.

Newman, A. J. 1996a. "Model Reduction via the Karhunen-Loeve Expansion Part I: An Exposition." Technical Report T.R.96-32, Institute for Systems Research, University of Maryland, Maryland.

Newman, A. J. 1996b. "Model Reduction via the Karhunen-Loeve Expansion Part II: Some Elementary Examples." Technical Report T.R. 96-32, Institute for Systems Research, University of Maryland, Maryland.

Ngoduy, D. 2011. "Multiclass First-Order Traffic Model Using Stochastic Fundamental Diagrams." *Transportmetrica* 7 (2): 111–125.

Prigogine, I., and R. Herman. 1971. *Kinetic Theory of Vehicular Traffic*. New York: Elsevier.

Richards, P. I. 1956. "Shock Waves on the Highway." *Operations Research* 4 (1): 42–51.

Schreckenberg, M., A. Schadschneider, K. Nagel, and N. It. 1995. "Discrete Stochastic Models for Traffic Flow." *Physical Review E* 51 (4): 2939.

Shu, C. W. 2006. "Essentially Non-Oscillatory and Weighted Essentially Non-Oscillatory Schemes for Hyperbolic Conservation Laws." In *Advanced Numerical Approximation of Nonlinear Hyperbolic Equations*, edited by A. Quarteroni, 325–432. Lecture Notes in Mathematics. Berlin, Heidelberg: Springer.

Shu, C. W. 2020. "Essentially Non-Oscillatory and Weighted Essentially Non-Oscillatory Schemes." *Acta Numerica* 29: 701–762.

Sirovich, L. 1987. "Turbulence and the Dynamics of Coherent Structures. I." *Coherent Structures." Quarterly of Applied Mathematics* 45 (3): 561–571.

Sumalee, A., R. X. Zhong, T. L. Pan, and W. Y. Szeto. 2011. "Stochastic Cell Transmission Model (SCTM): A Stochastic Dynamic Traffic Model for Traffic State Surveillance and Assignment." *Transportation Research Part B: Methodological* 45 (3): 507–533.

Wan, X., and G. E. M. Karniadakis. 2006. "Multi-Element Generalized Polynomial Chaos for Arbitrary Probability Measures." *SIAM Journal on Scientific Computing* 28 (3): 901–928.

Wang, Y., and M. Papageorgiou. 2005. "Real-Time Freeway Traffic State Estimation Based on Extended Kalman Filter: A General Approach." *Transportation Research Part B: Methodological* 39 (2): 141–167.

Wong, G. C. K., and S. C. Wong. 2002. "A Multi-Class Traffic Flow Model-an Extension of LWR Model with Heterogeneous Drivers." *Transportation Research Part A* 36: 827–841.

Xiong, T., M. Zhang, C. W. Shu, S. C. Wong, and P. Zhang. 2011. "High-Order Computational Scheme for a Dynamic Continuum Model for Bi-Directional Pedestrian Flows." *Computer-Aided Civil and Infrastructure Engineering* 26 (4): 298–310.

Xiu, D., and K. G. Em. 2003. "The Wiener-Askey Polynomial Chaos for Stochastic Differential Equations." *SIAM Journal on Scientific Computing* 24 (2): 619–644.

Xiu, D., D. Lucor, C. H. Su, and G. E. Karniadakis. 2002. "Stochastic Modeling of Flow-Structure Interactions Using Generalized Polynomial Chaos." *Journal of Fluids Engineering* 124 (1): 51–59.

Zhang, H. M. 2001. "New Perspectives on Continuum Traffic Flow Models." *Networks and Spatial Economics* 1 (1): 9.